Use of supramolecular interactions to control the self-assembly and properties of micellar gels

Bhaveshkumar BHARATIYA

Annual report - July 2012

1. Introduction

The PEO-PPO-PEO type triblock copolymers, commercially known as Pluronic[®], constitute an interesting class of amphiphiles due to their availability in a wide range of molecular weights and hydrophilic lipophilic balance (HLB).[1] The self-aggregation of Pluronic[®] block copolymers in a selective solvent, which is conducive for one block and poor for the other, gives rise to micelles with core-shell morphology.[2-6] The aqueous solution behavior of PEO-PPO-PEO triblock copolymers has been widely investigated in aqueous media. While the PEO block remains hydrophilic in water up to 100 $^{\circ}$C, the PPO block becomes hydrophobic after 15°C. The aggregation of PPO blocks above this temperature due to hydrophobic interaction is the driving force for the observed nanostructures.

The aqueous solution of some PEO-PPO-PEO block copolymer shows interesting rheological behavior and sol-gel transformation is observed at higher temperature. Chu and Zhou[7] observed dehydration of PEO blocks with increase in temperature, which was considered as the prime factor to induce gelation. Rassing et.al.[8] observed dehydration of the PPO core using ^{13}C NMR, which eventually results in enhanced friction among the polymer chains and increases the solution viscosity to end-up with gel formation. Different mechanisms have been proposed for the gelation of Pluronic solutions based on interaction and arrangement of the micelles in aqueous solutions. Wanka and coworkers[9] observed temperature induced gelation for 15wt% aqueous solutions of Pluronics (namely, P123, F127 and P104) above a certain characteristic value, where the temperature observed for sol-gel transition shifted to lower value with increase in concentration. Park et.al.[10] used SANS and rheology measurements to demonstrate two gel states for less hydrophilic P103 aqueous solutions, when the temperature was increased beyond phase separation. In this case, the first transition was attributed to the micellar growth and packing, while breaking of micelles due to dehydration of PEO blocks and resultant phase separation caused the sol-gel transition at higher temperatures. The composition of Pluronic block copolymers also plays a major role in deciding their gelation behavior. Kabanov et.al.[11] have shown that the aggregation of block copolymers increases with corresponding increase in temperature/concentration and when the aggregation number reaches a saturation, entanglement between hydrophilic PEO chains occurs due to deceased inter-micellar distance. Though, observed entanglement is highly dependent on the PEO molecular weight for a certain block copolymer. The formed

micelles can get packed through PEO entanglement provided PEO molecular weight exceeds a critical value of 1600 g.mol^{-1}.[12] Prud'homme and coworkers[13] using SANS and rheology have investigated the micellization and temperature induced gelation of Pluronic F127 in water. Chaibundit et.al.[14] investigated the gelation behavior of P123 in ethanol using SAXS and rheology. At higher copolymer concentration and below 30wt% ethanol addition, gels were formed due to packing of micelles in ether cubic or hexagonal array. The gel formation in the mixture of Pluronic F127 and P123 investigated using rheology reveals that the soft gels are transformed to hard gels and maxima is observed for micellar radius as the P123 proportion was increased in the mixture for the experimental temperature span.[15] Soni and coworkers[16] using small-angle X-ray scattering (SAXS), constructed the ternary phase diagram for P123 at 23°C and demonstrated formation of mixed cubic phase (face-centered cubic and hexagonally close-packed spherical micelles, fcc and hcp), a hexagonal phase (hex, cylindrical micelles), and a lamellar phase (planar micelles), when the concentration of copolymer was increased more than 30 wt % and at lower ethanol concentrations. In recent years, the application of gels based on PEO-PPO-PEO copolymers has been widely investigated especially in controlled drug delivery and other pharmaceutical formulations.[17-21]

By combining the polymer chemistry with metallo-supramolecular chemistry, the polymers that contain supramolecular binding units can be investigated for a possibility to develop several novel functional materials.[22,23] The metallo-supramolecular block copolymers and developed nanostructures in selective solvent by formation of metal-ligand complex has been investigated in detail.[24-29] The metal-ligand complexes based on the terpyridine have been explored to create large varieties of different supramolecular polymer architectures.[30,31] In our earlier report[32], metal-ligand interactions among terpyridine-modified PS-PtBA micelles lead to hierarchical supramolecular networks showing instantaneous recovery on applying mechanical stimuli. The obtained network was found strong chemical stimuli responsive and breaking of metal-ligand complex was noticed in presence of KCN, a strong competing ligand for Ni^{2+} and Fe^{2+} ions. We recently reported, the aqueous solution behavior of di (terpyridine) P105 and P123 in dilute regime.[33] At room temperature, the size population includes the micelles and aggregates of the micelles for di(terpyridine) P105, while only aggregates could be observed in case of di(terpyridine) P123. Addition of metal ions however disrupted partly the aggregates

and resulted in the formation of flower-like micelles due to di-terpyridine metal ions complexes in the micellar corona. These preliminary results prompted us to study terpyridine modified Pluronics in presence of transition metal ions in a more concentrated regime and as a function of temperature in order to promote the formation of micellar gels. To best of our knowledge, this is the first attempt to investigate metallo-supramolecular gels based on interaction of terpyridine modified Pluronics with added transition metal ion. The results are discussed in terms of the structural changes in aqueous solutions of modified Pluronics, as a result of formed complex and elevated temperature.

2. Materials and methods:

The PEO-PPO-PEO, Pluronic block copolymers F127 and P105 were purchased from BASF, Parsippany, NJ, USA. 4′-chloro-2,2′:6′,2″-terpyridine was a product purchased from Sigma-Aldrich. Dimethyl sulphoxide (DMSO) and toluene were analytical grade reagent from Sigma. Nickel chloride hexahydrate (NiCl$_2$.6H$_2$O), Pottasium hydroxide (KOH), Sodium chloride (NaCl) and sodium sulphate (Na$_2$SO$_4$), used either during organic reaction or sample preparation, were purchased from Aldrich. The aqueous solutions for dynamic light scattering (DLS) and rheology were prepared in milli-Q water. CDCl$_3$ (deuterated chloroform) for NMR and dimethyl formamide (DMF) for GPC were analytical grade regents obtained from sigma-aldrich.The synthesis of terpyridine modified Pluronic block copolymers was carried out as per our earlier report[33], finally characterized by NMR and GPC.

Dynamic light scattering (DLS):

DLS experiments were performed on a Malvern CGS-3 apparatus equipped with a He-Ne laser with a wavelength of 633 nm. The measurements were performed in water at 90° angle, and a concentration of 5 g · L^{-1}. The equilibration time was set to 30 min while changing the temperature of the analyzed sample. The data were analyzed using the CONTIN method, which is based on an inverse-Laplace transformation of the data and gives access to a size distribution histogram for the analyzed micellar solutions.

Rheology measurements:

The rheology measurements were carried out on Malvern Kinexus Ultra, stress controlled rotational shear rheometer. Sample was kept in a compartment comprising the plate-plate geometry. The temperature control enabled accurate temperature,

which was increased at 1 ^{o}C/min. The sample was kept under the shearing plate of 25 mm diameter. The gap height between the two plates was kept in range of 200-500μm. The frequency sweep measurements were carried out in range of 0.1-100 Hz. Rheology measurements as functions of temperature were carried out at 1 rad/sec frequency and 1 Pascal applied stress.

**Differential Scanning Caloriemetry (DSC):**

The Samples were examined for their thermal behavior in solutions using Mettler Toledo DSC 821e apparatus. An Aluminum sample cell was weighed accurately for sample weight in range of 5-10 mg. The sample was subjected to sine wave regulated heating programme with temperature increase at 1°C/min.

Sample Preparation:

For DLS measurements, the aqueous solutions of di(terpyridine) Pluronics were prepared by dissolving weighed amount of the sample in milli-Q water. The samples were kept in fridge at 4°C for a week to ensure complete solubility of the polymer blocks. The solutions were filtered with 0.2 μm PTFE filter, prior to the measurements. For Rheology, accurately weighed polymer sample was dissolved in milli-Q water and kept in fridge at 4°C for a week to insure complete solubility. Accurately weighed required amount of $NiCl_2.6H_2O$ was dissolved in water. The salt solution was drop-wise added to the polymer solution with constant stirring and desired concentrations of polymer and salt was maintained. The samples was then kept in tightly packed glass bottle for 3 days at the room temperature and stirred vigorously to insure homogeneous mixture. The accordingly obtained samples for di(terpyridine) F127 were highly viscous and optically clear, while marginal turbidity was noticed for di(terpyridine) P105 solutions.

3. Results and Discussion:

Aqueous solution behavior of di(terpyridine) Pluronics block copolymers in presence of $NiCl_2.6H_2O$ and salt free solutions, was attempted to investigate the molecular interactions at higher concentrations and metal-ligand complexation to promote supramolecular structures. In order to investigate the expected gel formation for di(terpyridine) Pluronics in water, a very hydrophilic block copolymer F127 (70% PEO, total M.W of 12600 g/mol) and P105 (50% PEO, 6500 g/mol, moderately hydrophobic) were selected.
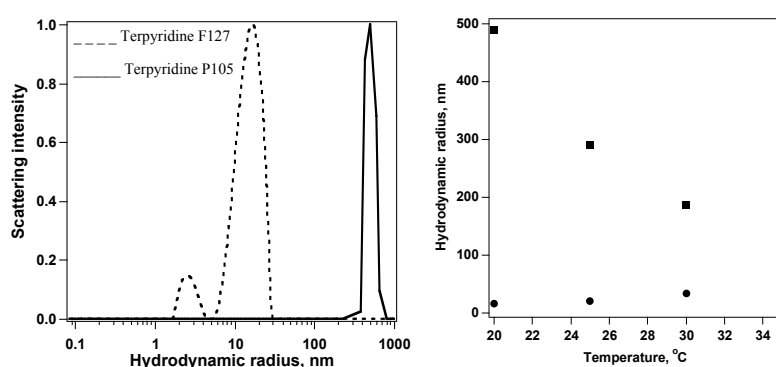

Figure 1. *(left) CONTIN size distribution histograms obtained for 5 mg.mL-1 aqueous solutions of Terpyridine Pluronics®, (right) Apparent hydrodynamic radii of 5 mg.ml-1 aqueous solutions of terpyridine F127 (●) and terpyridine P105 (■) versus temperature.*

Figure-1 (left) shows the hydrodynamic radius for 5 g.L^{-1} aqueous solutions of di(terpyridine) Pluronics at 20°C. The aqueous solution of di(terpyridine) F127 showed binomial distribution comprising fully extended unimers and micelles of 16 nm size. The aqueous solution of di(terpyridine) P105 showed presence of large size aggregate due to enhanced interaction between the terpyridine units at the coronal chains. In our earlier report[33] aqueous solutions of 0.1 g.L^{-1} solution measured for di(terpyridine) P105 showed presence of the mixture comprising micelles and aggregates of micelles at room temperature, while only aggregates were present at 30°C. A further increases of temperature results in turbid solution due to hydrophobic interactions between micelles caused by dehydration of blocks and presence of terpyridine ligand at PEO corona.

The evolution of the apparent hydrodynamic radii of the terpyridine F127 and terpyridine P105 was then followed as a function of temperature (Figure -1 (right)). In case of the F127 sample, a slight increase in the hydrodynamic radius versus temperature was noted. This could be due to the dehydration of F127 as temperature increases, resulting in an increase of the aggregation number of the micelles and hence in an increase of their overall size. On the other hand, a sharp

decrease of the apparent hydrodynamic radius was measured for the P105 sample. This could be due to the breaking of the terpyridine hydrophobic domains as temperature increases, as already observed before.[33]

Figure-2 (a) shows resultant changes in the G' (storage moduli) and G" (loss moduli) for 20% F127 aqueous solution. At frequency of 1 rad/sec and 1 Pascal of applied stress, the moduli values start to show an increase around 24°C. Further increase leads to crossover of the G' and G" curves, subsequently the Newtonian liquid is transformed to gel like viscoelastic material.
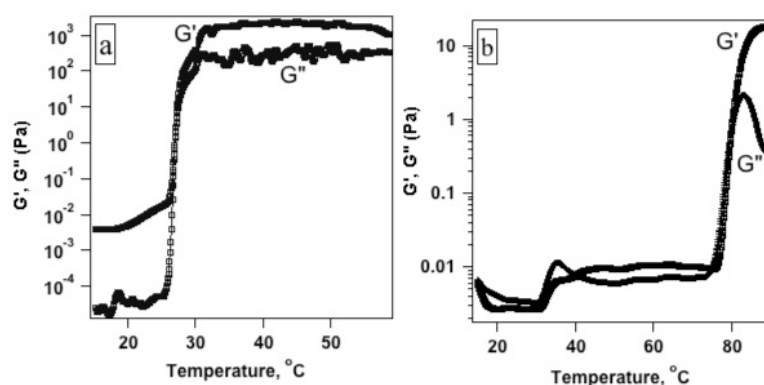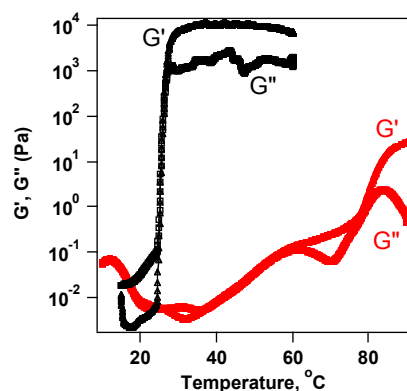

Figure 2: *G' (storage moduli) and G" (loss moduli) for 20% F127 (a) and 20% P105 (b) as a function of temperature.*

For very hydrophilic copolymer F127, the entanglement between the long PEO coronal chains drives the formation of viscoelastic network. The observed plateau modulus reaches value of 2.1×10^3 Pascal and remains constant for the measured temperature span. The 20% aqueous solution of P105 showed liquid-like behavior (G'<G") and phase separation caused by the dehydration of the PEO blocks could be evidenced with rise in moduli around 78°C.
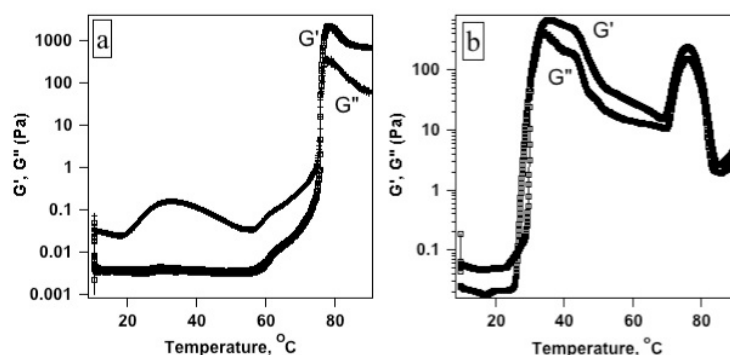

Figure 3: *G' (storage moduli) and G" (loss moduli) for 20% di(terpyridine) F127 (a) and di(terpyridine) P105 (b) as a function of temperature.*

Figure-3 shows changes in moduli for 20% di(terpyridine) Pluronic solutions subjected to shear stress as a function of temperature. The moduli values for di(terpyridine) F127 start to increase around 60°C and reaches to moduli values close to that observed for pure F127 case. The terpyridine ligand at the PEO corona adds to hydrophobicity of the system. Though terpyridine can be understood for the increased hydrophobic interaction between the micelles, it should have marginal effect to the corona entanglement. The solubility of the terpyridine units and dehydration of polymer chains at higher temperature is considered, but latter is more pronounced to affect the gelation. The observed fall in the moduli peak indicated phase separation caused by the complete dehydration of copolymer chains. The F127 aqueous solutions are highly soluble in water and shows cloud point (complete phase separation) above 100 ^{o}C. Due to increased hydrophobicity caused by terpyridine modification, phase separation occurs little below 100°C. The observed moduli does not reach plateau and seems to fall with further increase in temperature. Di(terpyridine) P105 sample showed a sudden jump in the G' around 30°C and observed increase is accompanied by cross-over of G' and G" curves. Plateau moduli for G' and G" were noticed at 700 and 450 Pa respectively. On further rise in the temperature, decrease of about a decade in the moduli values was observed. The moduli shows second successive rise around 68°C, which is an indication of the enhanced dehydration of the PEO blocks and resultant phase separation. It was interesting to note that unmodified P105 aqueous solution did not show the Initial jump in moduli as in this case. The observed phase separation for di(terpyridine) P105 aqueous solution was about 10°C prior, when compared to the unmodified sample. Park et. al.[10] studied the temperature induced two gel states of P103 micelles concluding that first maximum was initiated by the micellar packing, while the second maxima was the macroscopic liquid-liquid phase separation. The introduction of terpyridine at PEO corona could change the intermicellar interactions, which is reflected in the appearance of the maxima around 30°C. The observed results support the assumption that terpyridine modification enhances the hydrophobic interactions at the coronal chains and drives intermicellar interaction. Though, with considerably longer PEO corona the interactions are considerably weakened and can be understood by formation of clear solutions for di(terpyridine) F127.

Figure 4: *Changes in the storage moduli (G') and G"(loss moduli) as a function of temperature for 20% aqueous solutions of F127 (black) and P105(red) in presence of 0.5 equivalent Ni(II).*

The Pluronic solutions show remarkable phase behavior in presence of added salts, due to competition for hydration between the polymer blocks and the anions[2,6] or cations.[34,35] In order to understand possible effect of Ni(II) on polymer blocks, aqueous solutions of unmodified Pluronic were investigated in presence of Ni(II) ions. Figure-4 shows changes in the G' for 20% aqueous solution of Pluronics in presence of 0.5 equivalent of added nickel ions for the temperature ramp of 10-90°C. It was noticed that no significant changes were initiated in G' and G", when compared to salt free solution. The added concentration of chloride ions is not influential enough regarding competition with polymer blocks. It confirmed that low chloride concentration (least effective halogen member of Hoffmeister series) does not seem to disturb the hydration of polymer blocks.
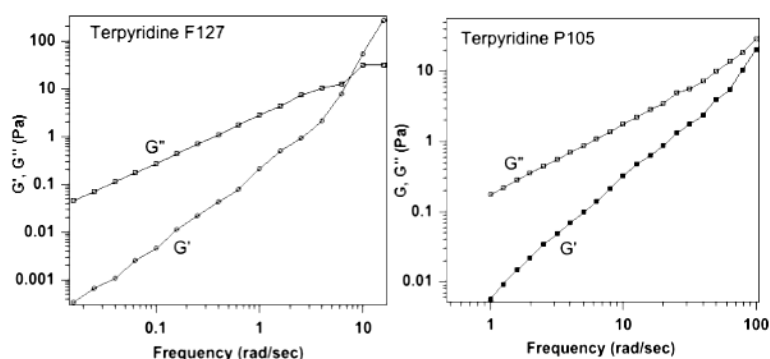
Figure 5: *Storage moduli (G') and loss moduli (G") for di(terpyridine) Pluronics in presence of 0.5 eq. Ni(II) as a function of applied frequency at 20°C*

The frequency sweep measurements for 20% di(terpyridine) Pluronic aqueous solutions in presence of 0.5 equivalent NiCl$_2$.6H$_2$O at 20°C are shown in Figure 5. The changes in the G' and G" at controlled stress of 1 Pascal and as a function of applied frequency (0.1-100 Hz) are shown. The logarithmic profile shows a decrease in the moduli values with a slope of -2 and -1 for G' and G", respectively. The

addition of Ni (II) ions to aqueous solutions of di(terpyridine) F127 and di(terpyridine) P105 is expected to results in metal-ligand interaction and complex formation at the PEO periphery. It can be concluded that the HLB ratio of these Pluronics is not significantly large compared to the PS-PtBA block copolymers examined in our previous study[33]. The terpyridine modified PS-PtBA aqueous solution resulted in formation of larger network, due to presence of micelles with longer corona, which ultimately hindered the hydrophobic interaction between the terpyridine units and favored interlinking of micelles through metal-ligand bis complex. In case of of 1 and 2 equivalent of $NiCl_2.6H_2O$, similar liquid-like behavior was observed (data not shown).
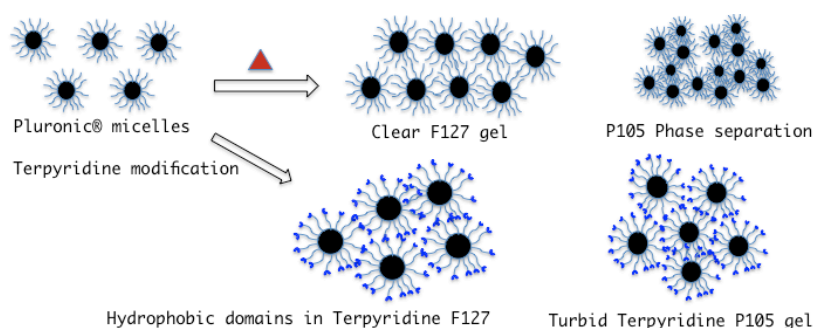
Scheme 1: *The interactions between the micellar aggregates driving to gel formation in metal –free state.*

In order to understand the effect of added Ni ions at higher temperature and resultant changes to network formation, we carried out measurements at higher temperatures.
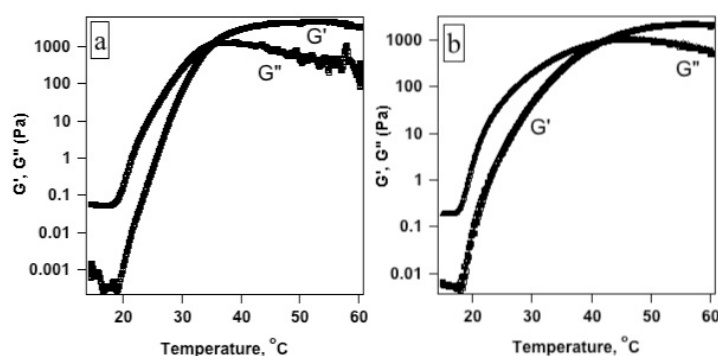
Figure 6: *Storage moduli (G') and loss moduli (G") for 20% aqueous solutions of di(terpyridine) F127 (a) and di(terpyridine) P105 (b) in presence of 0.5 equivalent Ni(II) as a function of temperature.*

Figure 6 shows the temperature scan for 20% di(terpyridine) Pluronics solutions in presence of 0.5 equivalent of Ni (II) ions. The sample subjected to 1 Pascal of applied stress and 1 rad/sec frequency, showed liquid-like behavior at 20°C. The clear transparent sample behaved like viscous fluid that starts to flow after a few

minutes. The addition of Ni ions to the terpyridine-modified solution is expected to initiate the metal-ligand interactions leading to the formation of mono/bis complex, which can be decided on the basis of interactions and availability of ions in the surroundings of the interacting terpyridine ligand. As the temperature is increased, the moduli value shows a moderate increase around 18°C. Even though, the formed network may be compared to chain extended polymer type, temperature induced increase in the moduli values is evident and is attributed to increased hydrophobicity of the PEO and PPO blocks. The observed value of G' becomes higher then G" after crossover of moduli curves around 34°C and attains a plateau around 38°C. The observed values of G' and G" are 4900 and 1200 Pa, respectively. The viscous moduli G" with value around 1000 Pascal, showed decrease after plateau was reached and could be attributed to the marginal solubility of terpyridine groups. The aqueous solutions of di(terpyridine) P105 in presence of 0.5 equivalent Ni ions at 20°C, was marginally turbid and viscous solution with G" higher than G'. With an increase in temperature a gradual rise in the moduli values was observed. The moduli curve crossover similar to di (terpyridine) F127 was observed. It should be noted that the observed trend is unique when compared to P105 aqueous solutions with and without modification. The metal introduction and resultant complex formation favors formation of supramolecular networks, which increase the moduli values. Though, the G" values remain higher than G' upto 35°C showing liquid-like behavior of the sample. The addition of metal-ion and resultant complex formation would diminish the hydrophobic interaction between the terpyridine groups at the corona, which is confirmed by the absence of first peak as observed for di(terpyridine) P105 aqueous solution. The observed values of G' and G" at the plateau are 2200 and 900, respectively. The lower plateau moduli values in comparison to di(terpyridine) F127 solution is attributed to the shorter PEO chains in P105 compared to F127. In fact, for di(terpyridine) F127 solution in presence of Ni ions, lesser corona interactions and higher degree of hydrophiliciity would facilitate the formation of clear gels at elevated temperatures. The observed gels in both case remained clear even up, to 75°C.
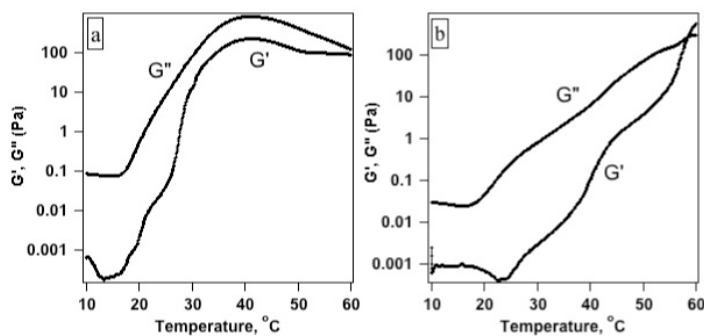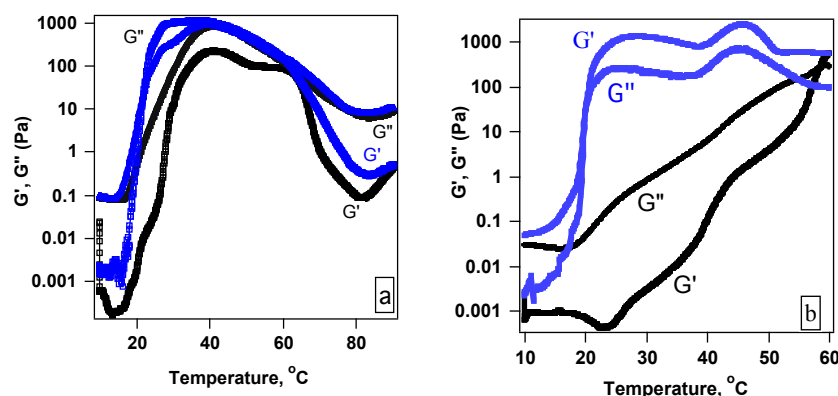
Figure 7: *Storage moduli (G') and loss moduli (G") for 20% aqueous solutions of di(terpyridine) F127 (a) and di(terpyridine) P105 (b) in presence of 0.5 equivalent Zn(II) as a function of temperature.*

Figure-7 shows chnages in G' and G" for 20% aqueous solutions of di(terpyridine) Pluronics in presence of Zn(II) ions. The moduli values start to show an increase around 18°C for Terpy-F127 case, but further increase does not induce cross-over of the moduli curves as observed for the Terpy-Pluronics in presence of Ni(II) ions. We conclude that the network formed with Zn(II) ions is weaker in comparison to that with Ni(II) ions. The G' and G" values increases almost paralelly to reach around 100 Pa and could be mainly attributed to the dehydration of the block, which only increases the viscosity. For the measured temperature span, the G" values remain higher that G', confirming the liquidlike behavior. In case of di(terpyridine) P105 aqueous solution in presence of Zn(II) ions, the moduli values shows an increase around 26°C and moduli cross-over was evidenced around 60°C. It can be concluded that Zn(II) ions play less influential role in promoting the gelation behavior. The absence of sol-gel transition could be the consequence of the weaker complex formation for Zn(II) case. The Ni(II) complex is stronger then Zn(II) showing crossover of the moduli after certain temperature.
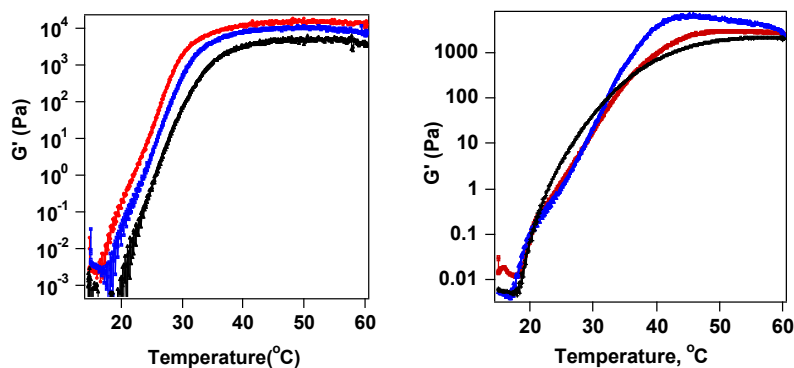
Figure 8: *Storage moduli (G') for 20% aqueous solutions of di(terpyridine) F127 (left) and di(terpyridine) P105 (right) in presence of defferent equivalents of Ni(II) as a function of temperature. 0.5 (black), 1.0 (red), 2.0 (blue)*

Figure-8 shows the changes in the storage moduli as a function of temperature for 20wt.% bis terpyridine Pluronics in presence of different equivalents of added Ni(II). For the bis(terpyridine) F127 case, the G' increases in amost identical manner to reach a value around 5000 pascal for the 1 eq. case at the plateau. For di(terpyridine) P105, the observed values for the G' increase with almost a similar value and reach to identical plateau. The observed values could be considered in the range of the error bar for the G', considering the evaporation of solvent during the sample handling and the increase in the temperature. Hence, the changes in the moduli values are considered to be independent of the added Ni(II). It was not possible to differentiate and elaborate the role of excess metal-ions to the complexation considering almost identical behavior observed for the measured samples.


Figure 9: *Storage moduli (G') for 20% aqueous solutions of di(terpyridine) F127 (a) and di(terpyridine) P105 (b) in presence of 0.5 equivalents of Zn(II) as a function of temperature. heating (black), cooling (blue)*

The heating-cooling cycles for the 20% bis(terpyridine) Pluronic in presence of Zn(II) are shown in Figure-9. The cooling cycles depict hysterysis and the curve returns to original moduli values at $10^{o}C$ ffor the cooling cycle. The hysterisis observed for Zn(II) added case was larger than that observed for the Ni(II) added case. The results again hint towards a gel behavior which is governed by the nature of added maetal ions and does not involve the structural rearrangement of the micelles as observed for the pure Pluronic case in general. The lack of large hysterisis and formation of clear gels suggest the gelation which is not governed at all by the micellar packing, rather the nature of the added metal-ion and hence the complexation.

In order to fully credit the results obtained by thermorheology, DSC measurements were carried out to examine the thermal behavior of the complexed samples. The

measurements for 10-90-10 heating-ccoling cycles for the bis(terpyridine),Pluronics in presence of 0.5 eq. Ni(II)/Zn(II) were measured by sine modulated temperature programme at $1^OC/min$.
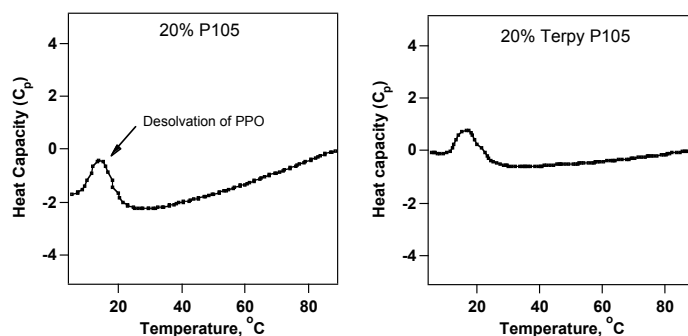
**Figure-10** *Modulated DSC thermograms showing complex heat capacity.*

Figure-10 shows the heat capacity for 20%P105 in modified and unmodifeied state. Pure P105 aqueous solutions showed an endothermic peak around 12^oC, which is attributed to the desolvation of the PPO blcoks, and refers to aggregation in form of nanostructures comprising PPO core surrounded by the PEO corona, for the case of Pluronics in solutions. For Terpy-P105 aqueous solutions, an identical endothermic transition was evidenced. Though, no thermal transitions could be evidenced at higher temperature. The obesrved transition is again attributed to the micelle formation with terpyridine decorated at the coronal chains.

Sokolov et.al.[36] have shown thermal transitions related to gelation for F127 aqueous solutions in presence of different additives. Recently, Titomanlio et.al.[37] reported endothermic transition corresponding to gelation for Pluronic aqueous solutions, where a very small peak was evidenced, a few degrees after the micellization peak. It was concluded that the energy required for the association of molecules in shape of micelles is comparatively larger than that required for gelation. In other words, less energy was required for the gelation once micelles were formed.
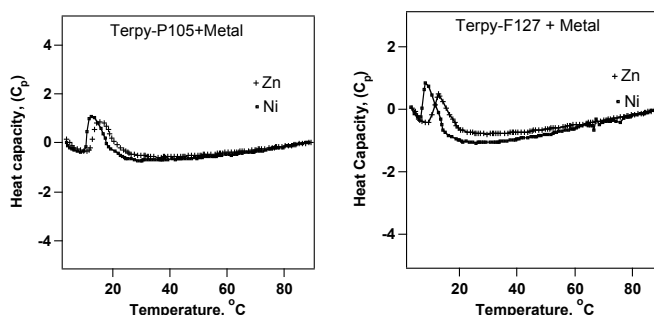
Figure-11 *Modulated DSC thermograms for aqueous solutions of terpy-Pluronics in presence of transition mtetal ion.*

As shown in Figure-11, the aqueous solutions of Terpy-P105 in presence of Ni(II) and Zn(II) showed similar endothermic transitions. The metal added samples were cooled at lower temperature and measured for the energy changes as a function of the applied temperature. At this stage, the complex formation at the PEO coronal chains yields formation of supramolecular network. Due to this reason, it was difficult to understand the exact intearctions envolving endothermic peak.
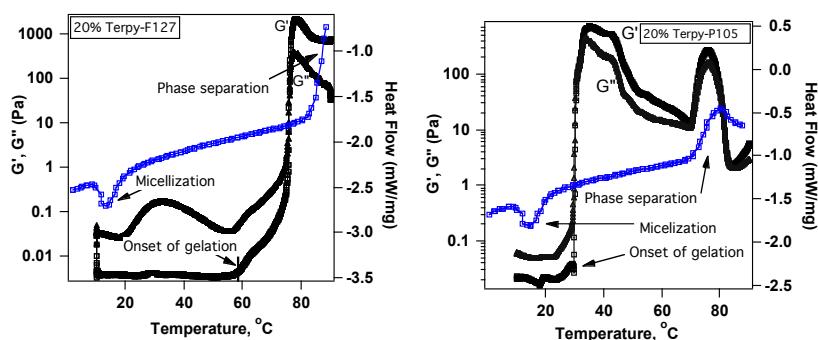
Figure 12: Thermorheology and DSC correlation plots for the di(terpyridine) Pluronics in presence of 0.5 eq. Ni(II)

The observed endothermic transition in Figure-10 could only be attributed to desolvation of PPO blocks. The polymer chains connected through complexation at the coronal chains, may experience hinderence to aggregate in spherical structure similar to non connected polymer chains. It was concluded that the transitions observed in rheology could not be directly correlated using thermal changes occuring in DSC.

4. References

1) Technical Brochure, Pluronic and Tetronic Surfactants, BASF Corp., Parsipanny, NJ (**1989**).
2) Chu B, Zhou Z. In Nonionic Surfactants; Marcel Dekker: New York, **1996**; Chapter 3, p 67.
3) Alexandridis P, Hatton TA. *Colloid Surf. A* **1995**, *96*, 1.
4) *Amphiphilic Block Copolymers: Self-Assembly and Applications*, Alexandridis P, Lindman B. Eds.; Elsevier: Amster- dam, **1997**.
5) Alexandridis, P. *Curr. Opin. Colloid Interface Sci.* **1997**, *2*, 478.
6) Nakashima K, Bahadur P. *Adv. Colloid Interface Sci.* **2006**, *123*, 75.
7) Zhou Z, Chu B. *J Colloids Interface Sci* **1988**, *126*, 171.
8) Rassing J, Mckenna W, Bandyopadhyay S, Eyring E. *J Mol Liq* **1984**, *27*, 165.
9) Wanka G, Hoffmann H, Ulbricht W. *Colloid Polym Sci* **1990**, *268*, 101.
10) Park MJ, Char K. *Macromol. Rapid Commun*. **2002**, *23*, 688.
11) Kabanov AV, Nazarova IR, Astafieva IV, Batrakova EV, Alakhov VY, Yaroslavov AA, Kobanov VA. *Macromolecules* **1995**, *28*, 2303.
12) Ferry JD, "*Viscoelastic Properties of Polymers*", 3rd edition, Wiley, New York **1989**.

13) Prud'homme RK, Wu G, Schneider DK. *Langmuir* **1996**, *12*, 4651.

14) Chaibundit C, Ricardo NM, Ricardo NM, Costa FM, Wong MG, Merino D, Rodriguez-Perez J, Hamley IW, Yeates SG, Booth C. *Langmuir* **2008**, *24*, 12260.

15) Chaibundit C, Ricardo N, Costa F, Yeates SG, Booth C. *Langmuir* **2007**, *23*, 9229.

16) Soni SS, Brotons G, Bellour M, Narayanan T, Gibaud A. *J Phys Chem B* **2006**, *110*, 15157.

17) Escobar-Chávez JJ, López-Cervantes M, Naïk A, Kalia YN, Quintanar Guerrero D, Ganem-Quintanar A.. *J Pharm Pharmaceut Sci* **2006**,9, 339.

18) Anderson B, Pandit N, Mallapragada S. *J Cont Rel* **2001**, *70*, 157.

19) He C, Kim S, Lee D. *J Cont Rel* **2008**, *127*, 189.

20) Xiong X, Tam K, Gan L. *J Nanosci Nanotech* **2006**, *6*, 2638.

21) Batrakova E, Kabanov AV. *J Cont Rel* **2008,** *130*, 98.

22) Beck JB, Rowan S. *J Am Chem Soc* **2003**, *125*, 13922.

23) Meier M, Schubert U. *Chem Commun* **2005**, *36*, 4610.

24) Gohy JF, Lohmeijer B, Varshney S, De'camps B, Leroy E, Boileau S, Schubert U. *Macromolecules* **2002**, *35*, 9748.

25) Gohy JF, Lohmeijer B, Schubert U. *Macromol Rapid Commun* **2002**, *23*, 555.

26) Gohy JF, Lohmeijer B, Schubert U. *Macromolecules* **2002,** *35,* 4560.

27) Guillet P, Fustin CA, Lohmeijer BG, Schubert U, Gohy JF. *Macromolecules* **2006**, *39*, 5484.

28) Guillet P, Fustin CA, Mugemana C, Ott C, Schubert U, Gohy JF. *Soft Matter* **2008**, *4*, 2278.

29) Mugemana C, Guillet P, Hoeppener S, Schubert U, Fustin CA, Gohy JF. *Chem Commun* **2010**, *46*, 1296.

30) Schubert U, Eschbaumer C. *Angew Chem* **2002**, *41*, 2892.

31) Schubert U, Eschbaumer C, Hien O, Andres P. *Tetrahedron Letters* **2001**, *42*, 4705.

32) Guillet P, Mugemana C, Stadler F, Schubert U, Fustin CA, Bailly C, Gohy JF. *Soft Matter* **2009**, *5*, 3409.

33) Chiper M, Hoeppener S, Schubert U, Fustin CA, Gohy JF. *Macromol Chem Phys* **2010**, *211*, 2323.

34) Radhakrishnan S, Schultz J. *J Crystal Growth* **1992**, *116*, 378

35) Liu L, Wan Q, Liu T, Hsiao B, Chu B. *Langmuir* **2002,** *18,* 104.

36) Jiang J, Li C, Lombardi J, Colby RH, Rigas B, Rafailovich MH, Sokolov JC. *Polymer* **2008**, *49*, 356.

37) Barba A, Amore M, Grassi M, Chirico S, Lamberti G, Titomanlio G. *J.Appl. Polym. Sci.* **2009**, *114*, 688.

Publication:

1). Supramolecular aqueous gels based on terpyridine modified Pluronics®
  Bhavesh Bharatiya, Charles-André Fustin, Jean-François Gohy

  Submitted to Macromolecular Chemistry and Physics

Supramolecular assembly of Poly(styrene)-*b*-Poly(4-vinylpyridine) and 6-Hydroxy 2-Naphthoic acid (HNA) in Thin film

1. Introduction:

The block copolymers in solution can form self-assembled structures of nanoscopic length scale, which has been an interesting topic among the researchers for few years now.[1-6] For application purpose, these block copolymers are used as thin films, where the structural behaviour could be more complicated compared to the bulk due to their interactions with underlying substrate. This class of ordered materials are applicable in the field of lithography, surface patterning, semiconducting nanomaterials and biosensing devices.[7-10]

A supramolecular control has been widely used approach for the fine-tuning of the block copolymer morphology in bulk[11,12] and thin films[13-15]. The idea of utilizing a small organic molecule, capable of forming association with either of the polymer blocks by weak forces of attractions like electrostatic interactions, van der Walls interaction and the hydrogen bonding has been investigated.[13-20] The associated small molecule can be removed by dissolution in selective solvent and nanoporous template can be obtained.[13] Such supramolecular control has been widely applied to the polystyrene-b-poly(4-vinylpyridine) (PS-P4VP) block copolymers, which are commercially available in large varieties of molecular weights. The strategy involves an interaction between the small organic molecule and vinyl pyridine (VP) group, leading to hydrogen bond formation. In this way, the introduction of the small molecule can alter the relative volume fraction of the each block and morphological changes are observed leading to varieties of hierarchical assemblies. The lateral ordering and morphology in the thin film are highly dependent on the nature of the solvent and the annealing environment.[21-24] The weak secondary bond between the VP block and the small molecule have shorter lifetime compared to the covalent bond and the strength of the same is dependent on the annealing environment and the presence of other molecules with stronger electronegative character.

The most commonly reported small molecule for such supramolecular interactions are 2-(4'-hydroxy benzeneazo)benzoic acid (HABA) and 3-pentadecylphenol (PDP). Most of the reports on supramolecular assembly involving PDP have been reported in the bulk. Tung and coworkers[15,24] and ten Brinke et.al[25] have investigated the structure-within-structure morphologies in thin films involving the interaction of PDP molecule with the 4VP group. Tung et al[15] have demonstrated

the correlation between the morphology orientation in thin films and the volume fraction of P4VP(PDP) block. ten Brinke and coworkers have reported the terrace formation in thin films comprising P4VP (PDP) supramolecular assembly.[25a] Stamm and coworkers have reported homogeneous thin films for the supramolecular assembly of PS-b-P4VP and a small organic molecule HABA containing two H-bonding groups.[10,13,26] The orientation of resultant cylindrical morphology could be switched to vertical or horizontal based on the solvent conditions. The dip-coated films from PS-P4VP containing HABA in THF showed the presence of mixture comprising vertical and horizontal cylindrical morphology.[13b] The morphology on the dip-coated thin films from 1,4-dioxane solution showed vertical cylinders comprising HABA(P4VP) surrounded by the PS matrix, while that from chloroform showed horizontal orientation. The switching of the morphology was realized by alteration of annealing solvent.[13,26] Nandan et.al have shown morphological changes in the film morphology by changing the P4VP/HABA molar ratio.[26c] Very few attempts have been made to investigate the interaction of PS-P4VP with a small organic molecule, other than the PDP and HABA. Kuila et.al reported the film morphology from PS-P4VP and 1-pyrenebutyric acid (PBA), where the cylindrical morphology changed to lamella for the dip-coated films from 1,4-dioxane solution.[10a] Prud'homme et al. investigated the thinfilms from PS-P4VP and mono-functional organic molecule 1,5-dihydroxy naphthalene (DHN) in THF solution, which leads to quasi-hexagonal nodular morphology.[14a] The depth of the nanopores obtained after washing the DHN in methanol, was a function of P4VP/DHN ratio and highest value was measured for 1:4 ratio. Recently, Bazuin et.al[27] used Naphthol and Naphthoic acid as a small molecule to influence the morphology changes by involving the interactions with 4VP block. It was noticed that with PS-P4VP/SM ratio of 1:1, the small molecule with −OH functionality leads to dot morphology while that with –COOH showed stripe morphology. Earlier similar changes to the film morphology were observed by Bazuin et al.[28] It was also demonstrated that the higher value of dip-coating rate, concentration and 4VP:SM ratio also lead to the stripe morphology.[27]

Table 1: Chemical structure of the organic molecule used for H-bonding with P4VP group

Name	Structure
6-Hydroxy-2-naphthoic acid **(HNA)**	
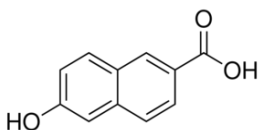
       We investigate on the SMA thin films of PS-P4VP and 6-hydroxy 2-Naphthoic acid (HNA) in 1,4-dioxane. The idea is to understand the effect of two functional groups on the film morphology in same base structure. The strength of the H-bonding between the small molecule and 4VP must be strong in order to have homogeneous film without exclusion of the small molecule from the thin film on to the surface. The already known stronger effect of -COOH group for H-bond formation than the –OH group prompted us to investigate the compound with both functional group, but with different base structure than that of HABA. The effect of concentration, annealing solvents, and pH will be attempted. The accordingly obtained nanotemplate can be used for the fabrication of metal nanoparticles. Our attempt will broaden the scope of using such supramolecular assembly based thin film morphology for application in nanoscience and nanotechnology.

2. Materials and methods:

The two poly(styrene-*b*-4-vinylpyridine) (PS4VP) block copolymer used in this study were purchased from Polymer Source Inc. and used as received. The small organic molecule 6-hydroxy 2- Naphthoic acid (HNA) was purchased from Sigma-Aldrich. The organic solvents 1,4-dioxane, THF, chloroform and methanol used in this study were purchased from Aldrich and filtered through 0.2 μm PTFE filter prior to the use. The molecular characteristics of the two block copolymers are shown in Table 1.

Table 2: Molecular characteristics of PS-P4VP block copolymers

Sample code	PS, M_n (g/mol)	P4VP, M_n (g/mol)	M_w/M_n	% P4VP
(A)PS$_{57.5}$-P4VP$_{18.5}$	57500	18500	1.12	24.3
(B)PS$_{22.0}$-P4VP$_{22.0}$	22000	22000	1.08	50.0

2.1 Preparation of solutions:

The accurately weighed required amount of PS-P4VP block copolymer and HNA were dissolved separately in 1,4-Dioxane by constant stirring for 3 hrs on magnetic stirrer. The solutions were then heated in the sonication bath at $80^{\circ}C$ for 2 hrs. The copolymer solution was drop-wise added to the small molecule solution under sonication at $80^{\circ}C$ in order to break the intra or inter-molecular H-bonds formed in the solution of small organic molecule HNA. The mixture was allowed to cool at the room temperature and kept overnight in order to insure the complete H-bonding between the P4VP group and the small molecule. The solutions were filtered with 0.2 μm PTFE filter prior to spin-coating procedure.

The Silicon substrates were cleaned by a piranha solution (H_2SO_4 98%/H_2O_2 30% 3/1) during 90 min. before being rinsed in ultra-pure water. The substrates were then dried with the spin-coater at a velocity of 4000 rpm for 20 s. Filtered solutions (0.2 μm) of mixtures in 1,4-Dioxane were then spin-coated onto these substrates at 2000 rpm during 40 s. The thickness of the films was controlled by the solution concentration and was evaluated by ellipsometry. The films were then annealed in 1,4-Dioxane vapors overnight. The schematic representation for the interactions involving PS-P4VP and HNA is shown below.
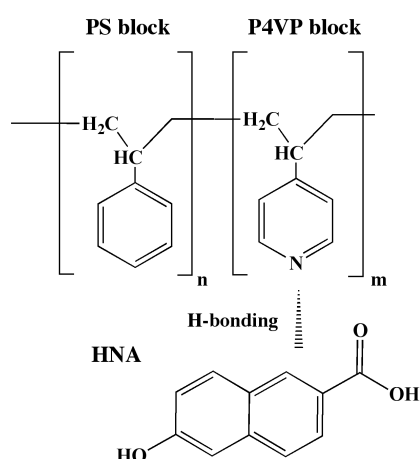
Scheme 1: Proposed H-bonding interactions between 4VP and HNA

To remove the small molecule, the thinfilms were immersed in methanol for 30 min and dried under nitrogen flow and then in a vacuum oven at 80 °C for 5 min to ensure complete methanol evaporation. The concentration of 1.0 wt.% copolymer was found to give a film of uniform thickness over the entire surface of the substrate for

equimolar SM:4VP compositions. Table-3 shows the composition of the supramolecular assembly (SMA) for the 1:1 mole ratio of P4VP/HNA.

Table 3: Composition of the SMA for the 1:1 mole ratio of P4VP/HNA.

Sample code	PS (g/mol)	P4VP (g/mol)	Weight Fraction	Morphology
S-(4VP-HNA)-0.473	57500	18500	0.473	D
S-(4VP-HNA)-0.736	22000	22000	0.736	D

HNA=6-hydroxy 2-Naphthoic acid, D=dot

2.2   Methods of Characterization:

Dynamic Light Scattering (DLS): The solution mixtures comprising desired PS-P4VP/HNA ratio, were filtered through 0.2 μm PTFE filter prior to the measurements. DLS experiments were performed on a Malvern CGS-3 apparatus equipped with a He-Ne laser with a wavelength of 633 nm. The measurements were performed in 1,4-dioxane at 90° angle, and at a concentration of 1 wt.%. The data were analyzed using the CONTIN method, which is based on an inverse-Laplace transformation of the data.

Atomic force Microscopy (AFM): Atomic force microscopy (AFM) was performed on a Digital Instruments Nanoscope IV scanning force microscope in tapping mode using NCL cantilevers (Si, 48 N/m, 330 kHz, Nanosenors).

Fourier Transform Infrared Spectroscopy (FTIR):

Infrared (IR) spectra were recorded in solution with a FT-IR spectrometer (Shimadzu FTIR-8400S). In case of ADCA, the compound was measured in pellet.

Results and Discussion:

Investigations on size and morphology in solution:

The PS-P4VP block copolymers are known to self-assemble in different organic solvents. The DLS measurements were performed in order to investigate the effect of added HNA molecule, which is expected to create hydrogen bonding with the 4VP block. Table-4 shows the measured hydrodynamic radius for 1 wt.% and 2 wt.% solutions of two PS-P4VP block copolymers with and without added HNA in 1,4-Dioxane at 90° angle. It was noticed that the block copolymer self assembles in micelles composed of the P4VP core and the PS corona, with typical size around 44

nm and 36 nm for PS(57500)-P4VP(18500) and PS(22000)-P4VP(22000) solution, respectively in 1,4-Dioxane. The measurements were extended at different angles and it was observed that the size was identical and independent of the angle of measurement (data not shown). The results confirm that the micelles are spherical and the size is identical within experimental uncertainty for a given copolymer whether or not the HNA is present. Bazuin[27] et.al have recently reported the thin films of PS-P4VP blocks with Naphthol and Naphthoic acid, where the micellar morphology was showing identical behavior. The unchanged size or shape of the PS-P4VP micelles is consistent with 1,4-Dioxane being a competitive H-bond acceptor, and thus the overall interactions do not enforce the morphological changes in solution.

Table 4: Hydrodynamic radius (R_h) and radius of two PS-P4VP block copolymers in 1,4-dioxane, with and without HNA

| Conc. (wt.%)	SM	PS(57500)-P4VP(18500)		PS(22000)-P4VP(22000)	
		R_h, nm	PDI	R_h, nm	PDI
	-	40.8±0.7	0.114	36.9±1.2	0.068
1	HNA	41.5±0.9	0.098	37.5±0.7	0.066
	-	44.4±1.1	0.233	37.3±0.6	0.119
2	HNA	44.7±0.6	0.196	37.5±0.3	0.092

The effect of concentration and the annealing solvent on pure PS-P4VP block copolymer:

In order to investigate the effect of HNA on block copolymer morphology in thinfilms, the two different concentrations of the block copolymer PS(57500)-P4VP(18500) in HNA-free solutions were spin-coated. The thin film morphology from 1wt.% and 2wt% concentrations in 1,4-Dioxane are shown in Figure 1(a) and 1(b), respectively.
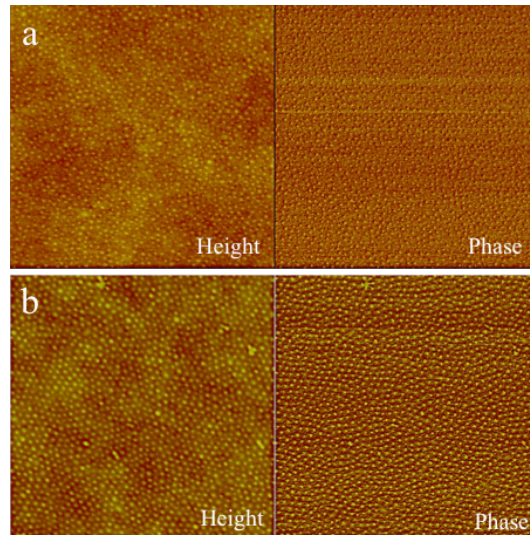
Figure 1: *AFM images of PS-P4VP thin film spin-coated on silicon substrate from 1 wt. % (a) and 2 wt.% (b) concentration in 1,4-dioxane (Scan size: 2 μm)*

The observed pattern shows dot morphology (nodules presumably of P4VP) that are roughly hexagonally arranged with periodicity. The films are annealed in 1,4-dioxane for 12 hrs prior to the AFM measurements. With change in the concentration, no changes to the dot morphology were observed. The formed morphology was similar in both cases, where the P4VP nodule remained vertically aligned. The measured diameters from 1wt% and 2 wt.% case were 17 and 18 nm, respectively. The centre – to-centre distance was around 45nm in both cases, while heights of the dots from the substrate were around 2 nm.
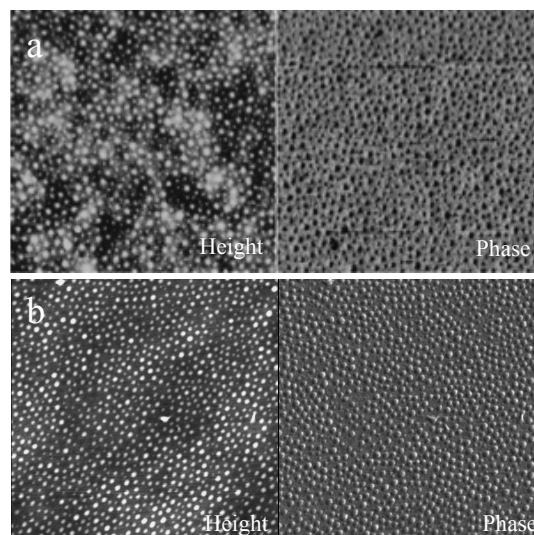
Figure 2: *AFM images of PS(57500)-P4VP(18500) from 1 wt.% annealed in (a) 1,4-dioxane and (b) chloroform (Scan size: 1.5 μm)*

The effect of annealing solvent on spin-coated substrate from 1wt.% PS(57500)-P4VP(18500) solution in 1,4-Dioxane is shown in Figure-2. The films were annealed in 1,4-dioxane and chloroform, in order to compare the effect of an oxygen bearing solvent and one without oxygen in it's structural composition. The presence of annealing solvent plays a major role in determining the structural arrangement and ordering of the morphology on thinfilm. [21-23] Recently, Tung et al.[24] investigated on the effect of annealing solvents on the morphological features of SMA comprising PS-P4VP and 3-Pentadecylphenol (PDP). It was noticed that in presence of oxygen bearing solvents, cylindrical morphology of PS cylinders was parallel to the surface. The same could be arranged perpendicular to the surface in presence of the non-oxygen bearing solvent like chloroform. The results in figure-2 reveal that P4VP morphology essentially remains as dot (spherical micellar core). The same was identical for chloroform-annealed case with no significant changes to the overall ordering and periodicity. The observed results confirmed that the PS(57500)-P4VP(18500) block copolymer remains as dot morphology for the annealed solvents under observation. To trigger morphological changes in the observed morphology, a small molecule HNA was added in equimolar proportion.

H-bond formation in supramolecular assembly comprising PS(57500)-P4VP(18500) and HNA:
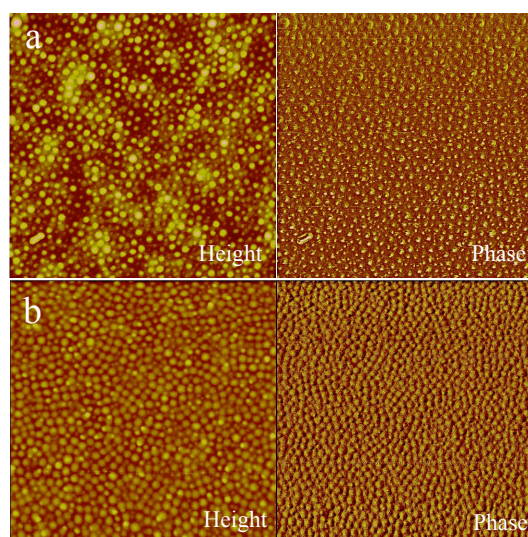
Figure 3: *AFM images for SMA thinfilm from HNA (a) as spun (b) annealed in 1,4-dioxane (Scan size: 2 μm)*

Figure-3 shows the AFM images for the spin-coated SMA films of PS-P4VP/HNA from 1,4-Dioxane solution. The addition of HNA results in hydrogen-bond formation between the P4VP block and –COOH/–OH group and thereby increases the volume fraction of the P4VP block. As shown in Figure-3(a), the as-spun thin films of SMA exhibited poor long range order of the self-assembled microdomains. The swelling of the SMA films deposited from 1,4-dioxane solution in vapors of this solvent affects the order of the microdomains. The thinfilm morphology shown in Figure-3(b) is well ordered and periodic after annealing in 1,4-Dioxane. Though, observed morphology in this case is dot (nodular) with increased diameter of ≈28 nm compared to ≈18 nm for pure PS-P4VP case. The increase in the size of the dot morphology confirms the H-bonding. The centre-to-centre distance between the neighbouring dots increases to ≈52 nm, which also accounts for the increase in the volume of P4VP dots. The addition of small molecule can alter the morphology on the thin film.[10,13,27] Laforgue et al.[14a] have shown that H-bond complexation between the small molecule Dihydroxy Naphthalene (DHN) and the block copolymer does not influence changes to the film morphology.

It should be noted that equimolar concentration of HNA combines with the P4VP block through H-bond complexation and increases the volume fraction of the P4VP block to 0.473, which is much higher than the boundary value for the transition corresponding to the lamellar morphology.[13] Though, the films spin coated from solutions of equimolar molar P4VP: HNA self-assemble into a quasi-hexagonal arrangement of dots comprising P4VP + HNA swollen above a PS matrix.
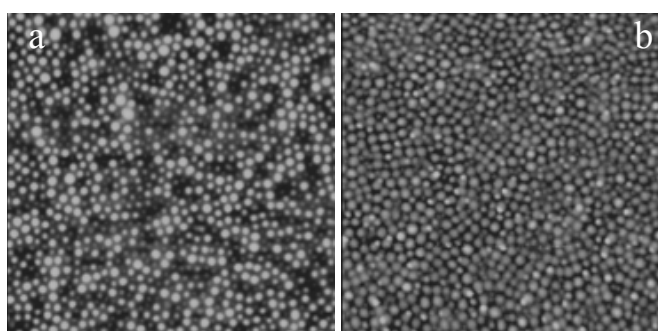
Figure 4: *AFM height images for SMA thinfilm from HNA annealed in (a) THF (b) 1,4-dioxane (Scan size: 2 μm)*

The thinfilm of SMA spin-coated from 1wt.% PS-P4VP/HNA solution in 1,4-Dioxane were annealed in THF in order to investigate the changes to the existing morphology. The Figure -4 shows the height images for the films annealed in THF

and 1,4-dioxane. The P4VP+ HNA block could be seen around PS matrix as a hexagonally arranged nodules in both case. The observed periodicity and geometric parameters for THF were roughly identical to that with 1,4-Dioxane. The size, centre-to-centre distance and height were 30, 50 and 11 nm, respectively. Though, the long-range periodicity was better in case of 1,4-dioxane annealed film compared to that in THF.
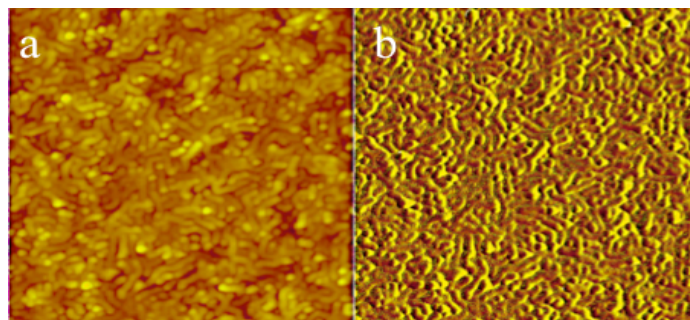
Figure 5: *AFM height (left) and phase (right) images for SMA thinfilm from 2wt.% solution in 1,4-dioxane. (Scan size: 3 μm)*

The concentration of spin-coating solution plays a major role in enforcing the morphological changes to the thin film. The recent study describes the transformation in the spherical film morphology to lamellar by increase in the solution concentration.[27] Figure-5 shows AFM image for spin-coated thinfilm of 2 wt.% (PS-P4VP + HNA) block copolymer in 1,4-Dioxane. The morphology changes to stripe-like from initial dot type as observed for 1 wt. case. The PS-P4VP + HNA oriented parallel to the surface was observed, though observed structures showed poor long-range order compared to the dot morphology for the 1wt. % case. The stripelike morphology on thin films was examined for the possibility to regain the dot structures by annealing in different solvents. The film was annealed in the chloroform and THF environment for 12 hrs. Though the film morphology was stripelike with no appearance of the dots.

The HNA molecule hydrogen bonded with the P4VP unit can be removed from the thinfilms by dissolution in selective solvent. Methanol is a better solvent for HNA and P4VP block, but not for PS. Figure-6 shows the AFM image for SMA thinfilms before and after washing in methanol. The Figure 6b shows that rinsing in methanol results in formation of nanoporous thinfilms. Methanol being poor solvent does not swell the PS phase. It was observed that the washing of HNA decreases the volume fraction of the PS-P4VP + HNA block keeping the actual structure in it's place.
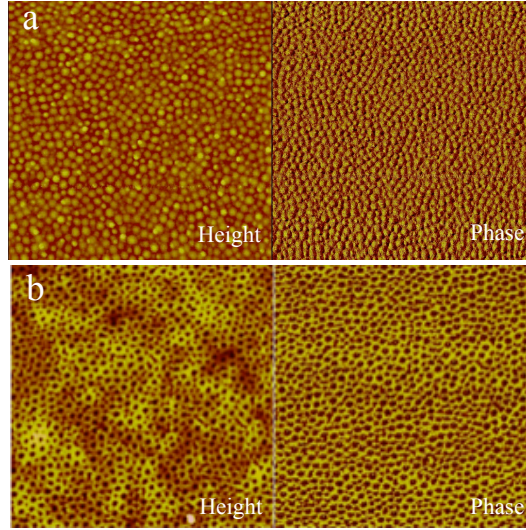
Figure 6*: AFM images for SMA thinfilm from HNA. (a) before rinsing in methanol (b) after rinsing in methanol (Scan size: 2 μm)*

The center-to-center distance for neighboring pores remained effectively same before and after the methanol washing. The average diameter and depth measured for the nanopores was ≈19 nm and ≈8 nm, respectively. Considering the respective molar volumes of 4VP and HNA, the observed values of the diameter for the pores is justified, which is roughly 2/3 times than that for the dots.

Table 5: Geometric parameters of the nanostructures in spin-coated PS-P4VP block copolymer films with and without HNA, before and after washing with Methanol

SMA thinfilm annealed in 1,4-Dioxane			
	$\boldsymbol{\theta}_{dot}$	$d_{p\text{-}p}$	h_{dot}
1 wt.% BC	17±3	45±6	3±1
2 wt.% BC	18±3	46±4	3±1
1 wt.% BC+HNA	28±4	52±6	10±2
[a]1 wt.% BC+HNA	30±5	50±5	11±3
After washing in Methanol			
	$\boldsymbol{\theta}_{pore}$	$D_{p\text{-}p}$	h_{pore}
1wt.% BC+HNA	19±5	49±7	8±3

$\boldsymbol{\theta}_{dot}$=diameter of dot, $d_{p\text{-}p}$=center-to -center distance between nearest dot, h_{dot} =height of dot above the matrix, $\boldsymbol{\theta}_{pore}$ =pore diameter, $D_{p\text{-}p}$ =center-to-center distance between nearest pores, h_{pore} =pore depth (All the measurements are in nm), a= in THF
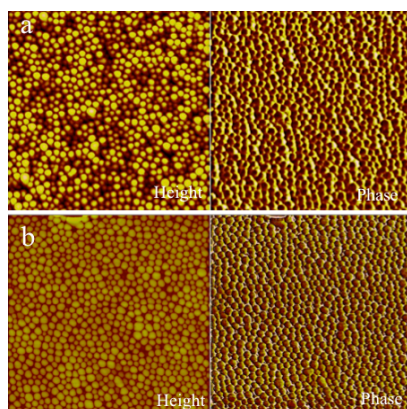
Figure 7: The AFM images for the thin films of 1 wt.% pure PS(22000)-P4VP(22000) (a) and mixed with HNA(b) in 1,4-dioxane solutions

To compare the film morphology in Figure-3 with different PS-P4VP block ratio, thin films were prepared from 1wt% equimolar mixture of PS(22000)-P4VP(22000) and HNA in 1,4-Dioxane. It contains 50 wt.% of P4VP, which is almost double to the PS(57500)-P4VP(18500) block copolymer. Figure-7 shows the AFM images of the thinfilms from the PS(22000)-P4VP(22000) with and without HNA. Figure-7(a) shows the spherical micelles poorly arranged in hexagonal array. After addition of HNA, the observed morphology showed improved long-range order and periodicity (Figure 7(b)). The analysis showed that the size and centre-to-centre distance between the neighbouring dots was almost unchanged. The results suggest that the H-bonding formation between the P4VP block and HNA was not complete and no increase in the volume fraction of the P4VP block occurred. As noted in some earlier reports, if the H-bond formation between the P4VP and SM is not strong enough, the compound may phase separate from the solution and crystallize on the surface during the spin coating or annealing procedure.

Supramolecular assembly from 4,4'-Azobenzenedicarboxylic acid (ADCA) and PS(57500)-P4VP(18500)

The compound 4,4'-Azobenzenedicarboxylic acid was obtained by the hydrolysis of corresponding hydrochloride. The azo compound 4,4'-Azobenzenedicarboxylic dichloride was purchased from Sigma-Aldrich. The measured solubility of this compound in different organic solvents was very low. The red-yellow colour powder was dissolved in THF and stirred overnight. Water was added drop-wise to this solution in a cooling bath with constant stirring. The mixture is stirred again for 4 hours to insure complete hydrolysis of the acid chloride. The resultant solution was transferred to separating funnel and dichloromethane is added. The mixture was vigorously shaken in order to facilitate the transfer of the product to the organic phase. Anhydrous Sodium sulphate was added in a very small amount to absorb the excess amount of water in the mixture. The solution is then filtered with 0.2 Nylon Milipore filter. After removing the solvent by distillation, a red colour compound was obtained which was characterized by FTIR as below. The structural characteristics of the final compound are as shown in the table below.
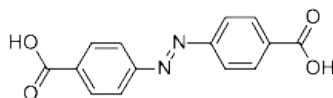

4,4'-Azobenzenedicarboxylic acid (ADCA)

The FTIR spectra clearly show the shift in the peak for the carbonyl group from 1734 to 1685 cm^{-1} indicating the hydrolysis and removal of –Cl by substitution of –OH. A broad peak around 2500-2900 cm^{-1} indicate the presence of –COOH group.
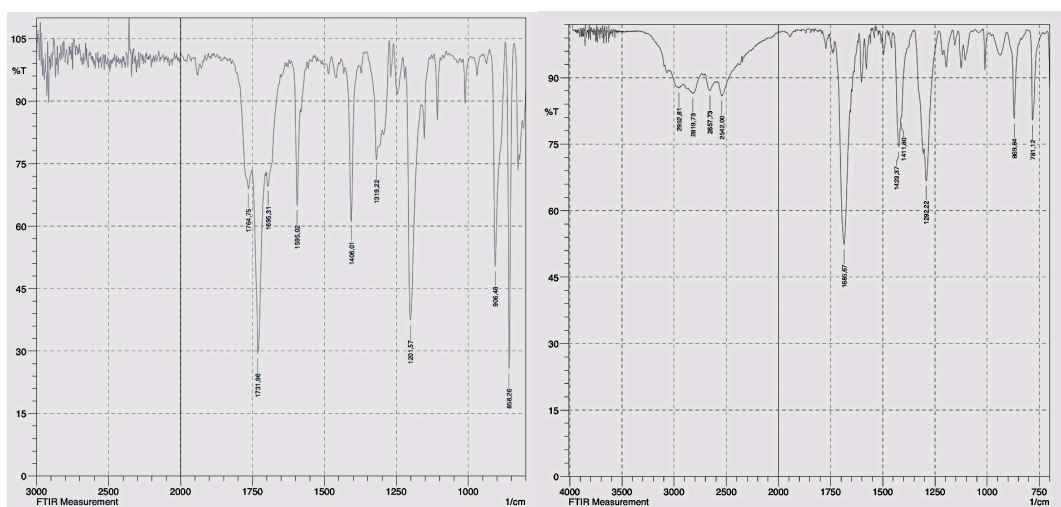
FTIR spectra for 4,4'-Azobenzenedicarboxylic chloride (left) and 4,4'-Azobenzenedicarboxylic acid (right)

The sample preparation was carried out as in case of SMA comprising HNA.
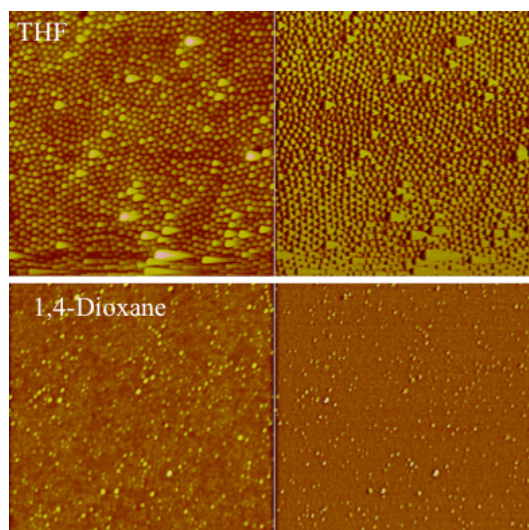
Figure 8: The AFM images for the thin films of 1 wt.% SMA solution of PS(57500) - P4VP(18500) mixed with equimolar amount of ADCA from THF and 1,4-dioxane solutions

The AFM images for SMA comprising PS-P4VP+ADCA showed essentially spherical dot morphology from 1,4-dioxane and THF solutions. The improved ordering and periodicity was observed with THF solutions. During the measurements, the crystallized ADCA molecules could be observed on the surface, indicating phase separation of the ADCA molecules from the P4VP block copolymer solution. Such observations indicate weak H-bond interactions between the P4VP and ADCA resulting into phase separation and no increase to the P4VP volume volume fraction. The obtained AFM images for the HNA case can be examined for the change in pH, which is expected to change the orientation of the P4VP at the pore walls. In case of HNA as SM, SMA mixtures with 1:2 and 1:4 ratio of P4VP: HNA were prepared, though AFM observations revealed that the small molecule crystallizes at the surface, hence the resultant morphology was not periodic and showed lack of uniformity.

References:

1) I.W. Hamley. The Physics of Block Copolymers; Oxford University Press: New York, 1998.
2) F.S. Bates, G.H. Fredrickson. *Phys Today* **1999**, *52*, 32
3) G. Krausch, R. Magerle. *Adv Mater* **2002**, *14*, 1579
4) F.S. Bates, G.H. Fredrickson. *Annu Rev Phys Chem* **1990**, *41*, 525
5) T. Thurn-Albrecht, J. Schotter, G.A. Kastle, N. Emley, T. Shibauchi, L. Krusin-Elbaum, K. Guarini, C.T. Black, M.T. Tuominen, T.P. Russell. *Science* **2000**, *290*, 2126

6) (a) M. Ramanathan, E. Nettleton, S.B. Darling. *Thin Solid Films* **2009**, *517*, 4474. (b) A. Knoll, A. Horvat, K.S Lyakhova, G. Krausch, G.J.A Sevink, A.V. Zvelindovsky, R. Magerle. *Phys. Rev. Lett.* **2002**, *89*, 035501

7) M. Park, C. Harrison, P.M. Chaikin, R.A. Register, D.H. Adamson. *Science* **1997**, *276*, 1401

8) N. Haberkorn, M.C. Lechmann, B.H. Sohn, K. Char, J.S. Gutmann, P. Theato. *Macromol. Rapid Commun.* **2009**, *30*, 1146

9) K.H. Lo, M.C. Chen, R.M. Ho, H.W. Sung. *ACS Nano* **2009**, *3*, 2660

10) (a) B.K. Kuila, E.B. Gowd, M. Stamm. *Macromolecules* **2010**, *43*, 7713 (b) B.K. Kuila, B. Nandan, M. Bohme, A. Janke, M. Stamm. *Chem Commun* **2009**, 5749 (c) B.K. Kuila, M. Stamm. *J Mater Chem* **2010**, 6086

11) O. Ikkala, G. ten Brinke, *Chem Commun.* **2004**, 2131

12) J. Ruokolainen, M. Saariaho, O. Ikkala, G. ten Brinke, E.L. Thomas, M. Torkkeli, R. Serimaa, *Macromolecules* **1999**, *32*, 1152

13) (a) I. Tokarev, R. Krenek, Y. Burkov, D. Schmeisser, A. Sidorenko, S. Minko, M. Stamm, *Macromolecules.* **2005**, *38*, 507 (b) A. Sidorenko, I. Tokarev, S. Minko, M. Stamm, *J Am Chem Soc* **2003**, *125*, 12211

14) (a) A. Laforgue, C.G. Bazuin, R.E. Prud'homme, *Macromolecules* **2006**, *39*, 6473. (b) C. Tang, E.M. Lennon, G.H. Fredrickson, E.J. Kramer, C.J. Hawker, *Science* **2008**, *322*, 429.

15) S.H. Tung, N.C. Kalarickal, J.W. Mays, T. Xu, *Macromolecules* **2008**, *41*, 6453

16) J. Ruokolainen, J. Tanner, G. ten Brinke, O. Ikkala, M. Torkelli, R. Serimaa, *Macromolecules* **1995,** *28*, 7779.

17) K.C. Wood, S.R. Little, R. Langer, P.T. Hammond, *Angew Chem., Int. Ed.* **2005**, *44*, 6704

18) C.F.J. Faul, M. Antonietti, *Adv Mater* **2003**, *15*, 673

19) A.F. Thunemann, *Prog Polym Sci* **2002**, *27*, 1473

20) (a) G.A. van Ekenstein, E. Polushkin, H. Nijland, O. Ikkala, G. ten Brinke, *Macromolecules* **2003**, *36*, 3684 (b) H. Kosonen, J. Ruokolainen, M. Knaapila, M. Torkkeli, R. Serimaa, W. Bras, A.P. Monkman, G. ten Brinke, O. Ikkala, *Synth Met* **2001**, *121*, 1277

21) Y. Xuan, J. Peng, L.Cui, H.F. Wang, B.Y. Li, Y.C. Han, *Macromolecules*, **2004,** *37*, 7301

22) H. Elbs, C. Drummer, V. Abetz, G. Krausch, *Macromolecule*, **2002**, *35*, 5570

23) J.K. Bosworth, M.Y. Paik, R. Ruiz, E.L. Schwartz, J. Huang, A.W. Ko, D.M. Smilgies, C.T. Black, C.K. Ober, *ACS Nano*, **2008**, *2*, 1396

24) W. Huang, P.Y. Chen, S.H. Tung, *Macromolecules* **2012**, *45*, 1562

25) (a)W. van Zoelen, T Asumaa, J. Ruokolainen G. O. Ikkala, ten Brinke, *Macromolecule* **2008**, *41*, 3199 (b) W. van Zoelen, S. Bondzic, T.F. Landaluce, J. Brondijk, K. Loos, A.J. Schouten, P. Rudolph, G. ten Brinke, *Polymer* **2009**, *50,* 3617

26) a) O. Seifarth, R. Krenek, I. Tokarev, Y. Burkov, A. Sidorenko, S. Minko, M. Stamm, D. Schmeisser. *Thin Solid Films,* **2007**, *515*, 6552. b) M. Bohme, B. Kuila, H. Schlorb, B. Nandan, M. Stamm. *Phys. Status. Solidi.* **2010**, *247*, 2458. c) B. Nandan, M.K. Vyas, M. Bohme, M. Stamm. *Macromolecules* **2010**, *43*, 2463

27) S. Roland, D. Gaspard, R. Prud'homme, C. Bazuin, *Macromolecules* **2012** doi.org/10.1021/ma3007398

28) A. Laforgue, D. Gaspard, C. Bazuin, R. Prud'homme, *Am.Chem.Soc.polym.prepr.* **2007**, *48*, 670